

Electrical transport through single-molecule junctions: from molecular orbitals to conduction channels

J. Heurich,¹ J.C. Cuevas,¹ W. Wenzel,² and G. Schön^{1,2}

¹*Institut für theoretische Festkörperphysik, Universität Karlsruhe, 76128 Karlsruhe, Germany*

²*Forschungszentrum Karlsruhe, Institut für Nanotechnologie, 76021 Karlsruhe, Germany*

(Dated: November 2, 2018)

We present an atomistic theory of electronic transport through single organic molecules that reproduces the important features of the current-voltage (I-V) characteristics observed in recent experiments. We trace these features to their origin in the electronic structure of the molecules and their local atomic environment. We demonstrate how conduction channels arise from the molecular orbitals and elucidate which specific properties of the individual orbitals determine their contribution to the current.

PACS numbers: 73.40.Jn, 73.40.Cg, 73.40.Gk, 85.65.+h

Introduction.— Present trends in the miniaturization of electronic devices suggest that ultimately single molecules may be used as electronically active elements in a variety of applications [1, 2]. Recent advances in the manipulation of single molecules now permit to contact an individual molecule between two electrodes (see Fig. 1) and measure its electronic transport properties [3, 4, 5, 6, 7, 8]. In contrast to single-electron transistors based on metallic islands [9], molecular devices have a more complicated, but in principle tunable, electronic structure. Interesting and novel effects, such as negative differential conductance [10], were observed in some of these experiments, which still, by-and-large, beg theoretical explanation. In addition to generic principles of nanoscale physics, e.g. Coulomb blockade [6, 11, 12], the chemistry and geometry of the molecular junction emerge as the fundamental tunable characteristics of molecular junctions [3, 4, 13, 14, 15, 16, 17].

In this paper we present an atomistic theory that bridges traditional concepts of mesoscopic and molecular physics to describe transport through single organic molecules in qualitative agreement with recent break-junction experiments [8]. We combine *ab initio* quantum chemistry calculations with non-equilibrium Green functions techniques to illustrate the emergence of *conduction channels* in a single-molecule junction from the molecular orbitals (MO). We further show how the specific properties of individual MOs are reflected in their contribution to the current. Using this data we provide insight into the microscopic origin of the nonlinear I-V characteristics observed experimentally and correlate their features to the specific properties of the molecule.

Our approach naturally accounts for the experimental observations and indicates that the current in these molecular junctions is mainly controlled by the electronic structure of the molecules and their local environment. We demonstrate that many molecular orbitals participate in a single conduction channel and provide examples where, surprisingly, the current is not dominated by the contribution from the energetically closest MOs. The

theory provides a quantitative criterion to judge the importance of individual MOs to the current and thus paves the way for the *a priori* design of molecular transport properties.

Theoretical model.— We calculate the current through a single molecule attached to metallic electrodes by a generalization of an earlier analysis of transport in atomic-size contacts [18], similar in spirit to Refs. [14, 17]. Since the conductance is mainly determined by the narrowest part of the junction, only the electronic structure of this “central cluster” must be resolved in detail. It is therefore sensible to decompose the overall Hamiltonian of the molecular junction as

$$\hat{H} = \hat{H}_L + \hat{H}_R + \hat{H}_C + \hat{V}, \quad (1)$$

where \hat{H}_C describes the “central cluster” of the system, $\hat{H}_{L,R}$ describe the left and right electrode respectively, and \hat{V} gives the coupling between the electrodes and the central cluster (see Fig. 1).

In this study the electronic structure of the “central cluster” is calculated within the density functional (DFT) approximation [19]. The left and right reservoirs are modeled as two perfect semi-infinite crystals of the corresponding metal using a tight-binding parameterization [20]. Finally, \hat{V} describes the coupling between the leads and the central cluster and takes the form: $\hat{V} = \sum_{ij} v_{ij} (d_i^\dagger \hat{c}_j + h.c.)$. The hopping elements v_{ij} between the lead orbitals d_i^\dagger and the MOs of the central cluster \hat{c}_j^\dagger are obtained by reexpressing the MOs of the central cluster via a Löwdin transformation in terms of atom-like orbitals, and then using the mentioned tight-binding parameterization [20].

The “central cluster” is not necessarily confined to the molecule, but may, in principle, contain arbitrary parts of the metallic electrode. The inclusion of part of the leads in the *ab initio* calculation was shown to improve the description of the molecule-leads coupling [15], in particular regarding charge transfer between the molecule and the electrodes. The Fermi energy of the overall system

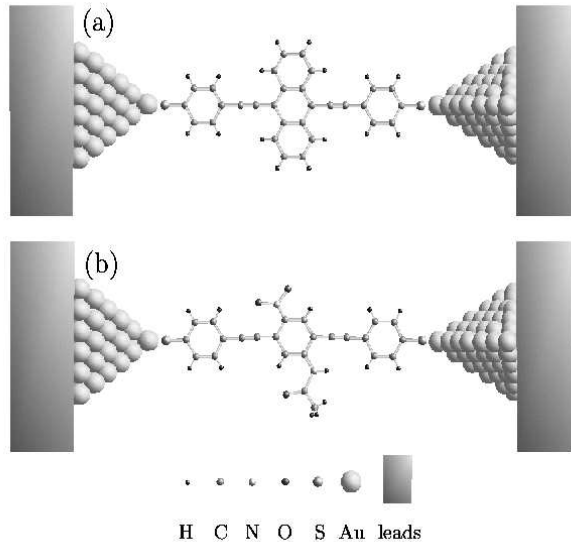


FIG. 1: Scheme of the single-molecule contacts analyzed in this work. The two organic molecules attached to gold electrodes, which were experimentally investigated in Ref. [8], are referred to as: (a) “symmetric molecule”, and (b) “asymmetric molecule”.

is determined by the charge neutrality condition of the central cluster.

In order to obtain the current for a constant bias voltage, V , between the leads, we make use of non-equilibrium Green function techniques. Since the Hamiltonian of Eq. (1) does not contain inelastic interactions, the current follows from the Landauer formula [21]

$$I = \frac{2e}{h} \int_{-\infty}^{\infty} d\epsilon \text{Tr} \{ \hat{t} \hat{t}^\dagger \} [f(\epsilon - eV/2) - f(\epsilon + eV/2)], \quad (2)$$

where f is the Fermi function and \hat{t} is the energy and voltage dependent transmission matrix given by

$$\hat{t}(\epsilon, V) = 2 \hat{\Gamma}_L^{1/2}(\epsilon - eV/2) \hat{G}_C^r(\epsilon, V) \hat{\Gamma}_R^{1/2}(\epsilon + eV/2). \quad (3)$$

The scattering rate matrices are given by $\hat{\Gamma}_{L,R} = \text{Im}(\hat{\Sigma}_{L,R})$, where $\hat{\Sigma}_{L,R}$ are the self-energies which contain the information of the electronic structure of the leads and their coupling to the central cluster. They can be expressed as $\hat{\Sigma}_{L,R}(\epsilon) = \hat{v}_{CL,R} g_{L,R}(\epsilon) \hat{v}_{L,R,C}$, \hat{v} being the hopping matrix which describes the connection between the central cluster and the leads. $g_{L,R}$ are the Green functions of the uncoupled leads (semi-infinite crystals), which are calculated using decimation techniques [22]. The Green functions of the central cluster are given by

$$\hat{G}_C(\epsilon, V) = \left[\epsilon \hat{1} - \hat{H}_C - \hat{\Sigma}_L(\epsilon - eV/2) - \hat{\Sigma}_R(\epsilon + eV/2) \right]^{-1}. \quad (4)$$

In order to provide a deep understanding of the electronic transport, we analyze the current in terms of *conduction channels*, defined as eigenfunctions of $\hat{t} \hat{t}^\dagger$. Such analysis allows to quantify the contribution to the transport of *every individual molecular level*. In our approach the channels arise as a linear combination of the molecular orbitals $|\phi_j\rangle$ of the central cluster, i.e. $|c\rangle = \sum_j \alpha_{cj} |\phi_j\rangle$, and the corresponding eigenvalues determine their contribution to the conductance. Ultimately, this information concerning the channels could eventually be measured using superconducting electrodes [23].

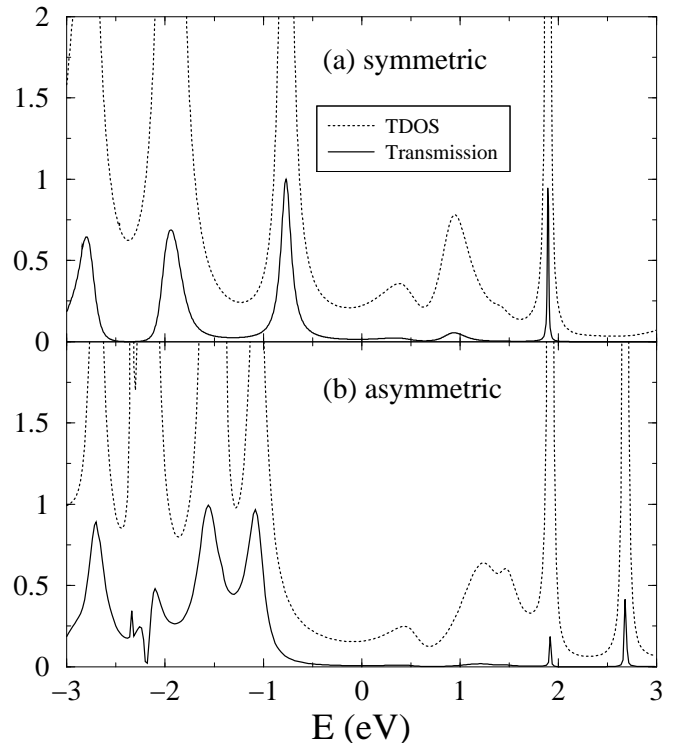


FIG. 2: Total density of states (TDOS) of the molecule and zero-bias total transmission as a function of the energy for both molecules. The Fermi energy is set to zero.

Results and discussions.— We now use the method described above to analyze the experiment of Reichert *et al.* [8]. The two organic molecules investigated are shown in Fig. 1, and as indicated in the caption, they will be referred to as symmetric and asymmetric molecule. For the description of the gold reservoirs, we use a basis with the atomic-like $5d, 6d, 6p$ orbitals, and for the central cluster we use the LANL2DZ basis [24] for all atoms. The DFT calculations were performed with the Becke three-parameter hybrid functional using the Lee, Yang and Parr correlation functional [25] at zero field [26]. In the calculations reported here one additional gold atom was included on either side of the molecule. Experimentally, both molecules were contacted several times and the nature of the I-V characteristics was found to vary with

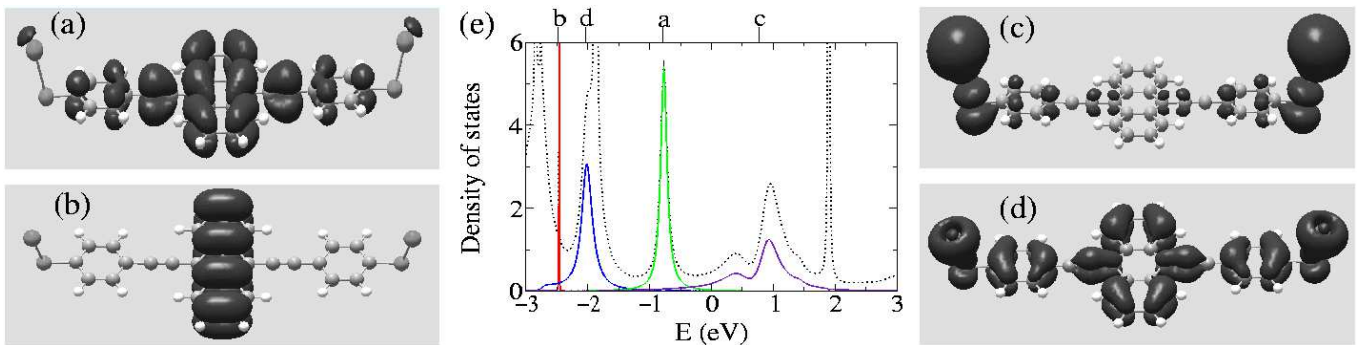


FIG. 3: (a-d) Charge-density plots of four molecular orbitals of the central cluster for the symmetric molecule. Panel (a) displays the HOMO and (c) the LUMO, which is twofold degenerate. (b) shows a confined orbital that contributes little to the current, while the MO in (d) is almost as important as the LUMO despite its difference in energy. Panel (e) shows the total density of states of the central cluster (dotted line) and the individual contributions of the four molecular orbitals (color lines). The level positions are indicated on top of this panel. The contributions of the different MOs to the conduction channel at the Fermi energy (set to zero) are: $|\alpha_a|^2 = 0.007$, $|\alpha_b|^2 = 10^{-11}$, $|\alpha_c|^2 = 0.06$, $|\alpha_d|^2 = 0.02$.

the quality of the contact. For this reason, theory can presently aim to elucidate important reproducible features of the experiment under the assumption that the contact to the electrodes is well defined. Since there is no direct experimental information regarding the geometry of the molecule and its attachment to the leads, the overall geometry of the central cluster was relaxed without additional constraints in our calculations, resulting

in the Au atom being out of the molecular plane.

Let us start by analyzing the linear response regime. In Fig. 2 we show for both cases the total density of states (TDOS) of the molecule and the zero-bias total transmission as a function of energy. As can be seen in the TDOS, in both cases the covalent bond between Au and S results in a strong hybridization between the molecular orbitals and the extended states of the metallic electrodes. The formation of wide energy bands and the disappearance of the gaps of the discrete molecular spectrum suggest the absence of Coulomb blockade in this type of molecular junctions.

The zero-bias total transmission as a function of energy follows closely the TDOS. The transmission is dominated overwhelmingly by a single channel in the energy window shown in Fig. 2, and the corresponding eigenvalues of $\hat{t}\hat{t}^\dagger$ at the Fermi energy [27] are $T_{sym} = 0.014$ and $T_{asym} = 0.006$. The decomposition of this channel into molecular orbitals provides us information on the relevance of the different molecular levels. Fig. 3 (a)-(d) show charge-density plots for some representative MOs and (e) shows their individual contribution to the TDOS. Fig. 3a shows that the highest occupied molecular orbital (HOMO) is confined to the interior of the molecule and its weight at the gold atoms is rather small. Consequently, in spite of its privileged energy position, the HOMO does not give a significant contribution to the current. The lowest unoccupied molecular orbital (LUMO), see Fig. 3c, exhibits the opposite behavior, i.e. it is very well coupled to the leads through the 6s atomic orbital of the gold atoms (notice that it has width of about 4 eV in the density of states), but the charge is mainly localized on the Au and S atoms. The interplay of these two factors yields a contribution of $\approx 6\%$ of the total current. Fig. 3(b,d) shows two further MOs with similar energy but very different contribution to the channel. While the localized MO (b) carries almost no current, the extended

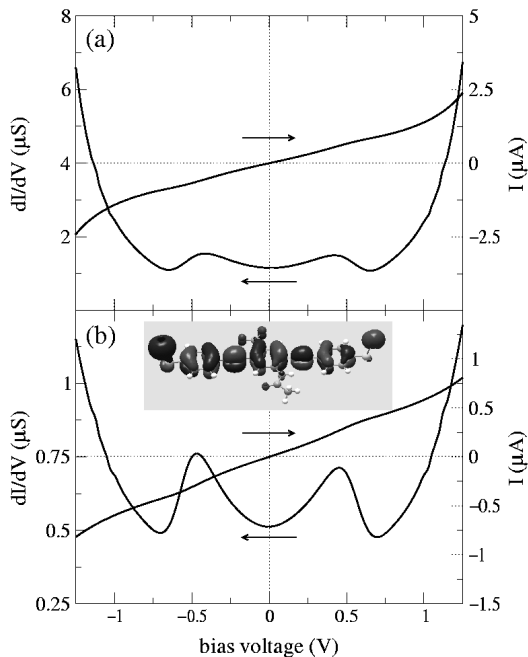


FIG. 4: I-V characteristics and differential conductance for the symmetric (a) and asymmetric (b) molecules. The inset in (b) shows the charge-density plot of the HOMO for the asymmetric molecule. Notice the intrinsic asymmetry of the charge distribution in the gold atoms.

and well coupled MO (d) has significant weight. Consequently there are three ingredients which determine the contribution of a MO to the current: (i) its energy position (distance to the Fermi energy), (ii) its bridging extent (whether it is extended or localized), and (iii) its coupling to the leads. Our analysis provides a counterexample to the conventional wisdom that the HOMO and the LUMO dominate the transport properties.

Fig. 4 shows the I-V curves for both molecules in the voltage range investigated in Ref. [8]. Both the order of magnitude and shape of the current and conductance agree qualitatively with the experimental results. There is no pronounced voltage dependence of the transmission due to the smooth density of states of the gold electrodes in the energy region explored here. The nonlinearities in these I-V curves can be then understood by a simple inspection of the energy dependence of the zero-bias transmission. For instance, the pronounced increase in the conductance around 1 V is due to the fact that we approach the resonant condition for the HOMO and LUMO.

In agreement with the experiment, the I-V of the symmetric molecule is symmetric with respect to voltage inversion, while the one of the asymmetric molecule is asymmetric. According to Eq. 2 we note that the asymmetry of the MO is not a sufficient condition for an asymmetric I-V characteristic, as evidenced by the experimental I-V near zero bias. Only the energy dependence of the left/right scattering rates in Eq. 3 induces an asymmetry into the I-V characteristic. Such asymmetries can arise either from differences in the local atomic structure of the electrodes or from intrinsic properties of the molecule. The latter arise from the asymmetric charge distribution of the MOs (see inset Fig. 4b), resulting in different couplings to the leads. Even for the symmetric molecule, we were able to induce asymmetries into the I-V characteristic by distorting the geometry of one of the lead fragments in the central cluster. This fact was nicely demonstrated in the experiment (see Fig. 5 in Ref. [8]). We investigated several other scenarios regarding the number of gold atoms, their geometry and the coupling and found predictable variations of the I-V's with these changes. If, for example, the gold-sulfur bond is stretched by about 5%, the current changes by about 70%, but the position of the peaks in the conductance and their peak/valley ratios are only marginally affected.

Conclusions.— We have presented an atomistic semi-quantitative description of non-linear transport through a single molecule junction. We were able to attribute distinctive features of the I-V's of the symmetric and asymmetric molecule to their individual molecular levels ob-

tained from *ab initio* calculations. The resolution of conductance into conduction channels permits an analysis of the contributions of individual orbitals to overall transport. In this way we provide an understanding which can be valuable for the future engineering of molecular devices.

We are grateful for many stimulating discussions with D. Beckmann, M. Hettler, M. Mayor, H. Weber and F. Weigend. The work is part of the CFN which is supported by the DFG. JCC acknowledges funding by the EU TMR Network on Dynamics of Nanostructures, and WW by the German National Science Foundation (We 1863/10-1), the BMBF and the von Neumann Institute for Computing.

-
- [1] *An Introduction to Molecular Electronics*, edited by M.C. Petty, M.R. Bryce (Oxford Univ. Press, New York, 1995).
 - [2] For recent reviews see C. Joachim, J.K. Gimzewski, A. Aviram, *Nature* **408**, 541 (2000); A. Nitzan, *Annu. Rev. Phys. Chem.* **52**, 681 (2001).
 - [3] C. Joachim *et al.*, *Phys. Rev. Lett.* **74**, 2102 (1995).
 - [4] S. Datta *et al.*, *Phys. Rev. Lett.* **79**, 2530 (1997).
 - [5] M.A. Reed *et al.*, *Science* **278**, 252 (1997).
 - [6] C. Kergueris *et al.*, *Phys. Rev. B* **59**, 12505 (1999).
 - [7] D. Porath *et al.*, *Nature* **403**, 635 (2000).
 - [8] J. Reichert *et al.*, cond-mat/0106219.
 - [9] *Single Charge Tunneling*, edited by H. Grabert and M. Devoret (Plenum Press, New York, 1992).
 - [10] J. Chen *et al.*, *Science* **286**, 1550 (1999).
 - [11] U. Banin *et al.*, *Nature* **400**, 542 (1999).
 - [12] H. Park *et al.*, *Nature* **407**, 57 (2000).
 - [13] E.G. Emberly and G. Kirczenow, *Phys. Rev. B* **58**, 10911 (1998).
 - [14] S.N. Yaliraki *et al.*, *J. Chem. Phys.* **111**, 6997 (1999).
 - [15] M. Di Ventura, S.T. Pantalides and N.D. Lang, *Phys. Rev. Lett.* **84**, 979 (2000). M. Di Ventura *et al.*, *Phys. Rev. Lett.* **86**, 288 (2001).
 - [16] J. Taylor, H. Guo and J. Wang, *Phys. Rev. B* **63**, 121104 (2001); **63**, 245407 (2001).
 - [17] J.J. Palacios *et al.*, *Phys. Rev. B* **64**, 115411 (2001).
 - [18] J.C. Cuevas, A. Levy Yeyati and A. Martín-Rodero, *Phys. Rev. Lett.* **80**, 1066 (1998).
 - [19] GAUSSIAN98 (Rev. A9), M.J. Frisch *et al.*, Gaussian Inc. Pittsburgh, PA, 1998.
 - [20] D.A. Papaconstantopoulos, *Handbook of the band structure of elemental solids*, Plenum Press, New York (1986).
 - [21] R. Landauer, *IBM J. Res. Develop.* **1**, 223 (1957).
 - [22] F. Guinea *et al.*, *Phys. Rev. B* **28**, 4397 (1982).
 - [23] E. Scheer *et al.*, *Nature* **394**, 154 (1998).
 - [24] P.J. Hay and W.R. Wadt, *J. Chem. Phys.* **82**, 299 (1985).
 - [25] A.D. Becke, *J. Chem. Phys.* **98**, 5648 (1993).
 - [26] Additional DFT calculations at fixed electric field showed resulted in no significant differences in the voltage range explored here.
 - [27] We chose the Fermi energy in the middle of the HOMO/LUMO gap and verified that for the molecules investigated here the transmission at the Fermi energy is not very sensitive to this choice.